Thermoconvective instabilities in a horizontal porous annulus with an external wavy wall

Jabrane Belabid
Laboratory of Mathematics and Applications, Faculty of Sciences and Technologies, University Hassan II, P.O. Box 146, Mohammedia, Morocco

(Received 17 April 2019; published 8 October 2019)

This paper investigates the thermal instability in a horizontal porous annulus with an external wavy wall. The porous matrix is supposed to be filled by an incompressible fluid. The model that we consider includes the heat equation and the hydrodynamics equations under the Darcy law and Boussinesq approximation. The derived model with the temperature-stream function is solved numerically using the alternating direction implicit method. Our numerical results indicate that the heat transfer and the convective instability depend strongly on the waviness of the external cylinder. The results of this paper confirm that the heat transfer is enhanced when the waviness amplitude increases. It is noticed that the thermoconvective instabilities are strongly affected by the undulation number.

DOI: 10.1103/PhysRevFluids.4.103501

I. INTRODUCTION

Natural convection heat transfer in a porous medium has gained increased attention during the last several decades. This interest is mainly due to its wide range of practical applications in modern industry and engineering, such as compact heat exchangers, solar power collectors, geothermal energy systems, cooling of nuclear reactors, movement of contaminants in groundwater, food industries, and crude oil extraction, to name just a few.

The literature indicates that convection heat transfer inside a concentric annulus arises in multiple applications in science and engineering, such power plant steam lines, buried electrical cables, oil and gas transmission lines, and cryogenics. During the last few years, a large number of papers have dealt with free convection in a horizontal porous annulus. Reference [1] was the first to study the problem experimentally and numerically. The author used the Christiansen effect to visualize the isotherms of radius ratio $R = 2$ and determined experimentally a different Nusselt number. The perturbation technique was also used to obtain a two-dimensional steady-state solution. Numerous other studies include Refs. [2–6], and recently Ref. [7] showed that at relatively high Rayleigh numbers, thermal instabilities appear as steady counterrotating cells in the upper part of the annulus. A similar behavior was observed for small gap widths.

Moreover, many studies on wavy-walled rectangular or square enclosures have been reported in the literature. Reference [8] used the finite element technique based on the Galerkin method to solve the problem of natural convection inside a porous cavity with a sinusoidal vertical wavy wall. Reference [9] analyzed the effect of volumetric heat sources on natural convection in a wavy-walled cavity. These authors found that the heat transfer rates depend mainly on the value of the wavy walls' amplitude. Reference [10] used the finite element method to analyze numerically the heat transfer from a vertical wavy wall in a porous cavity. The author found that the convection process is sensitive to the Rayleigh number, wave amplitude, wave phase, and number of waves. His results showed that small sinusoidal drifts from the smoothness of a vertical wavy wall with a phase angle of 60° and high frequency seem to enhance the heat transfer. Reference [11] used the Forchheimer-Buongiorno approach to simulate the effect of thermal dispersion on the heat transfer inside a porous

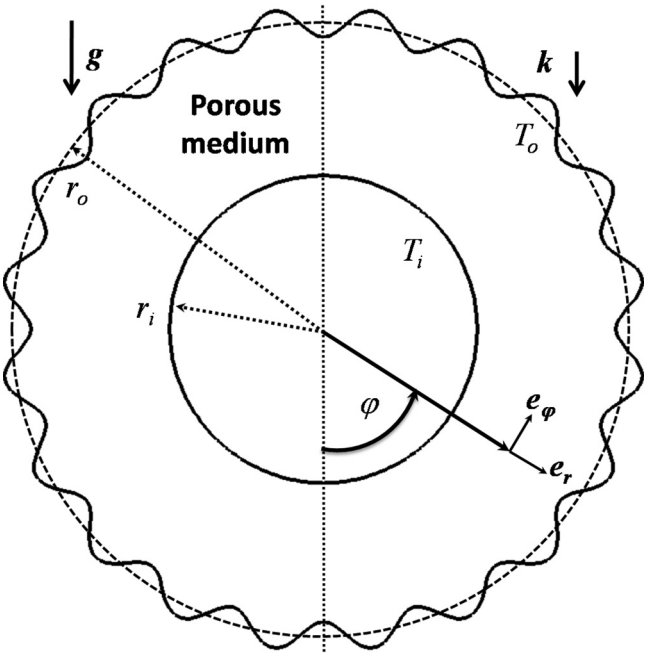

FIG. 1. Schematic of the problem and coordinate system.

wavy cavity filled with a nanofluid. The results proved that an increase in the undulation number leads to a significant attenuation of the convective flow. It has been revealed, also, that the heat transfer is more pronounced for relatively high undulation numbers. Reference [12] used a response surface method (RSM) in combination with the finite element method to investigate convective heat transfer of nanofluids in a wavy absorber collector. The RSM analysis shows that the best case for the wavy wall implicates the possible smallest wave amplitude in an average wave number. More recently, Ref. [13] used a Dupuit-Forchheimer model to analyze the convective heat transfer flow of nanofluid in a porous medium over a wavy surface. Their results illustrate that the injection of nanoparticles enhances the heat transfer rate.

The main objective of this paper is to investigate natural convection heat transfer in a horizontal porous annulus with a wavy cold wall. According to the author's best knowledge, this problem has not been treated yet. The rest of the work is organized as follows. The mathematical formulation is given in the next section. The numerical methods are presented in Sec. III, followed in Sec. IV by discussion of some numerical data. The work is concluded in the last section.

II. PROBLEM DESCRIPTION AND MATHEMATICAL FORMULATION

The problem treated here is a porous layer saturated with an incompressible Newtonian fluid and bounded by a horizontal concentric inner flat cylinder of radius r_i and wavy outer cylinder. The wavy wall of the enclosure is described by the relation $r_{\text{wavy}} = r_o(1 - \lambda \cos 2\eta\varphi)$, where r_o is the radius of the outer flat cylinder, λ is the amplitude of the sinusoidal profile, and η is the number of undulations. The considered domain of interest is presented in Fig. 1. Both inner and outer cylinders are kept at uniform, constant, and different temperatures T_i and T_o, respectively, with $T_i > T_o$. It is taken into account that the flow is two-dimensional, steady, and laminar.

The porous medium is considered to be homogeneous. Under the Boussinesq approximation, the basic steady conservation of thermal energy, momentum, and mass equations in polar coordinates

system can be written as

$$(\rho C_p)_m \frac{\partial T^*}{\partial t^*} + (\rho C_p)_f (\mathbf{V}^* \cdot \boldsymbol{\nabla}) T^* = k \nabla^2 T^*, \tag{1}$$

$$\mathbf{V}^* = -\frac{K}{\mu}[\boldsymbol{\nabla} P^* + \rho_0 g \beta (T^* - T_o)], \tag{2}$$

$$\boldsymbol{\nabla} \cdot \mathbf{V}^* = 0. \tag{3}$$

The boundary conditions are as follows:

(1) On the inner cylinder surface ($r^* = r_i$): $u^* = v^* = 0,\ T^* = T_i$

(2) On the outer cylinder surface ($r^* = r_{wavy}$): $u^* = v^* = 0,\ T^* = T_o$

where T^* is the temperature, V^* is the velocity, P^* is the pressure, K is the permeability, μ is the dynamic viscosity, ρ_0 is the reference density, β is the coefficient of thermal expansion, and g is the gravitational acceleration. The heat capacity of the saturated porous medium is considered equivalent to $(\rho C_p)_m = \epsilon(\rho C_p)_f + (1-\epsilon)(\rho C_p)_s$ where ϵ and ρ stand, respectively, for porosity and fluid density. The subscript m designates the fluid-solid mixture, and subscripts f and s refer, respectively, to the fluid properties and the solid matrix. k is the equivalent thermal conductivity.

To obtain the dimensionless model, we introduce the following scales: r_i for distance, $r_i^2(\rho C_p)_m/k$ for time, $k/r_i(\rho C_p)_f$ for velocity, ΔT for temperature, and $k\mu/K(\rho C_p)_f$ for pressure. Therefore, the dimensionless governing equations can be rewritten as

$$\frac{\partial T}{\partial t} + (\mathbf{V} \cdot \boldsymbol{\nabla}) T = \nabla^2 T, \tag{4}$$

$$\mathbf{V} = -\boldsymbol{\nabla} P - \mathrm{Ra} T k, \tag{5}$$

$$\boldsymbol{\nabla} \cdot \mathbf{V} = 0, \tag{6}$$

where k is the unit vector oriented vertically downward ($k = \frac{g}{||g||}$), Ra is the Rayleigh number given by $\mathrm{Ra} = \frac{g\beta K \Delta T r_i (\rho C_p)_f}{k\nu}$, ν is the kinematic viscosity, and $\Delta T = T_i - T_o$ is the temperature difference.

The dimensionless boundary conditions are as follows:

$$\begin{aligned} &u = v = 0, \quad T = 1 \text{ on } r = 1, \\ &u = v = 0, \quad T = 0 \text{ on } r = R\,(1 - \lambda \cos 2\eta\varphi), \end{aligned} \tag{7}$$

where $R = \frac{r_o}{r_i}$ is the flat cylinders' radius ratio. Due to the physical symmetry of the problem the following boundary conditions are added:

$$\varphi = 0, \quad \pi : v = 0, \quad \frac{\partial T}{\partial \varphi} = 0. \tag{8}$$

The governing equations for the laminar natural convection in terms of stream function-temperature formulation can be expressed as follows:

$$\nabla^2 \psi = -\mathrm{Ra}\left(\sin\varphi \frac{\partial T}{\partial r} + \frac{\cos\varphi}{r}\frac{\partial T}{\partial \varphi}\right), \tag{9}$$

$$\frac{\partial T}{\partial t} + \frac{1}{r}\frac{\partial \psi}{\partial \varphi}\frac{\partial T}{\partial r} - \frac{1}{r}\frac{\partial \psi}{\partial r}\frac{\partial T}{\partial \varphi} = \nabla^2 T, \tag{10}$$

where the stream function is defined by

$$V = \left(\frac{1}{r}\frac{\partial \psi}{\partial \varphi}, -\frac{\partial \psi}{\partial r}\right). \tag{11}$$

The corresponding boundary conditions take the following form:

$$\begin{aligned} &r = 1 : T = 1 \text{ and } \quad \frac{\partial \psi}{\partial \varphi} = 0, \\ &r = R\,(1 - \lambda \cos 2\eta\varphi) : T = 0 \text{ and } \quad \psi = 0, \\ &\varphi = 0, \pi : \frac{\partial T}{\partial \varphi} = \psi = 0. \end{aligned} \tag{12}$$

The local Nusselt number along the inner cylinder is estimated as the ratio of convective to conductive heat transfer:

$$\mathrm{Nu}_i(r = 1, \varphi) = -\ln R \left.\frac{\partial T}{\partial r}\right|_{r=1}, \tag{13}$$

and the average Nusselt number evaluated at the inner cylinder can be written as

$$\overline{\mathrm{Nu}} = \frac{1}{S}\int_0^S \mathrm{Nu}_i \, ds, \tag{14}$$

where S stands for the length of the wall formed by the inner cylinder.

III. NUMERICAL METHODS AND CODE VALIDATION

The mathematical problem along with boundary conditions was solved by the second-order finite difference method using a nonuniform mesh for the radial coordinate. The discretized stream function and energy equations were solved with the alternating directions implicit method. The Thomas algorithm in conjunction with iterations was used to solve the resulting matrix systems. The time limit for solution of the transient problem is considered as the steady-state solution. It should be noted that there are many ways for choosing the initial conditions that can be introduced in the computations. The initial conditions used in this work are the same as in Ref. [7]. Hence, as initial conditions, the stream function is set to zero everywhere. However, the value of the temperature is given as

$$T = 1 - \frac{\log r}{\log R}\sum_{m=1}^{M}\sum_{n=0}^{N} b_{mn} \sin\left(m\pi \frac{\log r}{\log R}\right)\cos(n\varphi), \tag{15}$$

where m and n stand, respectively, for the number of discretization points in the r-φ directions. As presented in Refs. [14,15], the conduction heat transfer represented by $1 - \frac{\log r}{\log R}$ induces a unicellular flow pattern, while the establishment of bicellular or multicellular flow regimes requires that $b_{i,j} = 0$ except for $b_{1,6} = -0.3$, $b_{1,7} = 0.3$, $b_{1,8} = -0.3$, and $b_{1,7} = 0.3$. The iteration process is terminated when the following criterion is satisfied in each node of the grid:

$$\max \left| \frac{\xi_{i,j}^{n+1} - \xi_{i,j}^{n}}{\xi_{i,j}^{n}} \right| < 10^{-8}, \tag{16}$$

where ξ designates T or ψ, the subscript i and j indices denote grid location in the (r, φ) plane, and n refers to the iteration number.

The present model, in the form of an in-house code, has been validated against the other published data for the case of concentric flat cylinders for $R = 2$ and $\mathrm{Ra} = 50, 100$. The comparison is shown in Table I where a good agreement is observed.

For the purpose of obtaining a grid-independent solution, a grid independence analysis is conducted. In fact, numerical tests, using various mesh grids, were examined in order to determine the best compromise between the grid-independent solutions and the calculation time. The results in terms of average Nusselt number along the hot wall of the annulus for $R = 2$, $\mathrm{Ra} = 100$, $\lambda = 0.03$,

TABLE I. Average Nusselt number for $R = 2$ and $\lambda = 0$ and comparison with literature.

	Grid size	Ra = 50	Ra = 100
[1]	49 × 49	1.328	1.829
[16]	25×25	1.362	1.902
[17]	30 ×44	1.335	1.844
[6]	10×10	1.341	1.861
[5]	10×10	1.341	1.861
[18]	50×50	1.342	1.835
[4]	30×95	1.344	1.867
[19]	161×101	1.338	1.861
[20]	10×18	1.317	1.865
[21]	100×240	1.343	1.868
[22]	50×50	1.3455	1.8752
This study	49×49	1.343	1.851

and $\eta = 10$ are presented in Table II. On the basis of the performed verifications, the structured grid of 300 × 300 points has been selected for the further investigation.

IV. RESULTS AND DISCUSSIONS

Numerical analysis of the boundary value problem (9)–(12) has been carried out at the following key parameters: radius ratio $R = 2$, Rayleigh number Ra = 50–100, amplitude of sinusoidal profile $\lambda = 0$–0.45, and number of undulations $\eta = 0$–50. Particular efforts have been focused on the effects of these parameters on heat transfer characteristics and thermoconvective instabilities.

Figure 2 illustrates the effect of undulation number on the average Nusselt number. It is revealed that the maximum convective heat transfer rate on the inner cylinder is observed at $\eta = 1$, and then the average Nusselt number decreases gradually with the increase of undulation number. This figure shows that an increase of the amplitude λ leads to an intensification of the convective flow.

As presented in previous works [2,7], different flow regimes may develop depending on the initial conditions used in the computation, the thickness of the annulus, and the value of the Rayleigh number. In fact, thermoconvective instabilities appear by the development of additional convective cells on the top of the annulus. Results show that, exceeding a threshold, a small perturbation of the Rayleigh number leads to the development of a new branch of solutions where the flow pattern structure is bicellular. This phenomenon called the bifurcation is generated by the thermoconvective instabilities. The bifurcation point is characterized by the critical value of the Rayleigh number Ra_c

TABLE II. Mesh effect on the average Nusselt number of the hot wall for $R = 2$, Ra = 100, $\lambda = 0.03$, and $\eta = 10$.

Grid size	$\overline{\mathrm{Nu}}_{i\times j}$	$\frac{\overline{\mathrm{Nu}}_{i\times j}-\overline{\mathrm{Nu}}_{401\times 401}}{\overline{\mathrm{Nu}}_{401\times 401}} \times 100\%$
31 × 31	1.9923	0.6415
101 × 101	1.9804	0.0404
151 × 151	1.9800	0.0202
201 × 201	1.9798	0.0101
251 × 251	1.9797	0.0051
301 × 301	1.9797	0.0051
401 × 401	1.9796	–

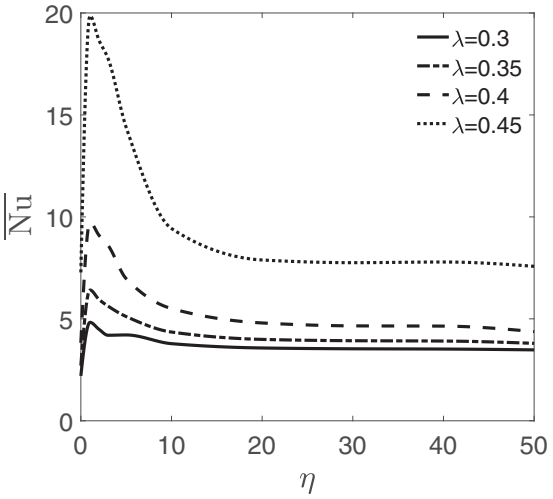

FIG. 2. Average Nusselt number as function of η for Ra = 100 and different values of λ.

under which the bicellular flow regime transits towards a unicellular one (see Refs. [2,4,5,7]). The first step of the numerical determination of the bifurcation point consists of obtaining a bicellular flow pattern by considering a relatively high value of Rayleigh number. Then this latter value is gradually decreased until the unicellular flow structure is met.

For a flat horizontal porous annulus, the bifurcation point is determined at $\mathrm{Ra}_c = 62.4$ (Fig. 3). Therefore, the flow transits from a unicellular flow structure for Ra = 62.4 towards a bicellular one where a second cell appears in the top of the annulus for Ra = 62.5. The cells are contrarotative. These data are in good agreement with the already published results. In fact, Ref. [6] determined the bifurcation point between the unicellular and bicellular flow regimes at $\mathrm{Ra}_c = 65.5 \pm 0.5$. Reference [15] found that this flow regime transition occurs at $\mathrm{Ra}_c = 67$. This result has been validated further by the results of Ref. [4], which define the bifurcation point at $60.5 < \mathrm{Ra}_c < 61.5$. Moreover, the results obtained by Refs. [5,21] have determined numerically the flow regime transition as $\mathrm{Ra}_c = 62$.

Our numerical simulations show that the flow pattern depends mainly on the waviness of the outer cylinder. Hence, the unicellular-bicellular regime transition is highly affected. Figure 4 illustrates that, for $\eta = 30$, the two-dimensional unicellular-bicellular regime transition occurs at Ra = 62.8, Ra = 63.4, Ra = 64.1, and Ra = 65.6 when λ equals 0.05, 0.15, 0.2, and 0.25, respectively.

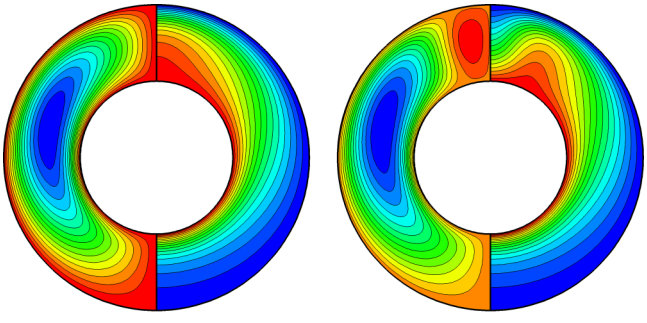

(a) : Ra = 62.4 (b) : Ra = 62.5

FIG. 3. Streamlines (left) and isotherms (right) for $\lambda = \eta = 0$.

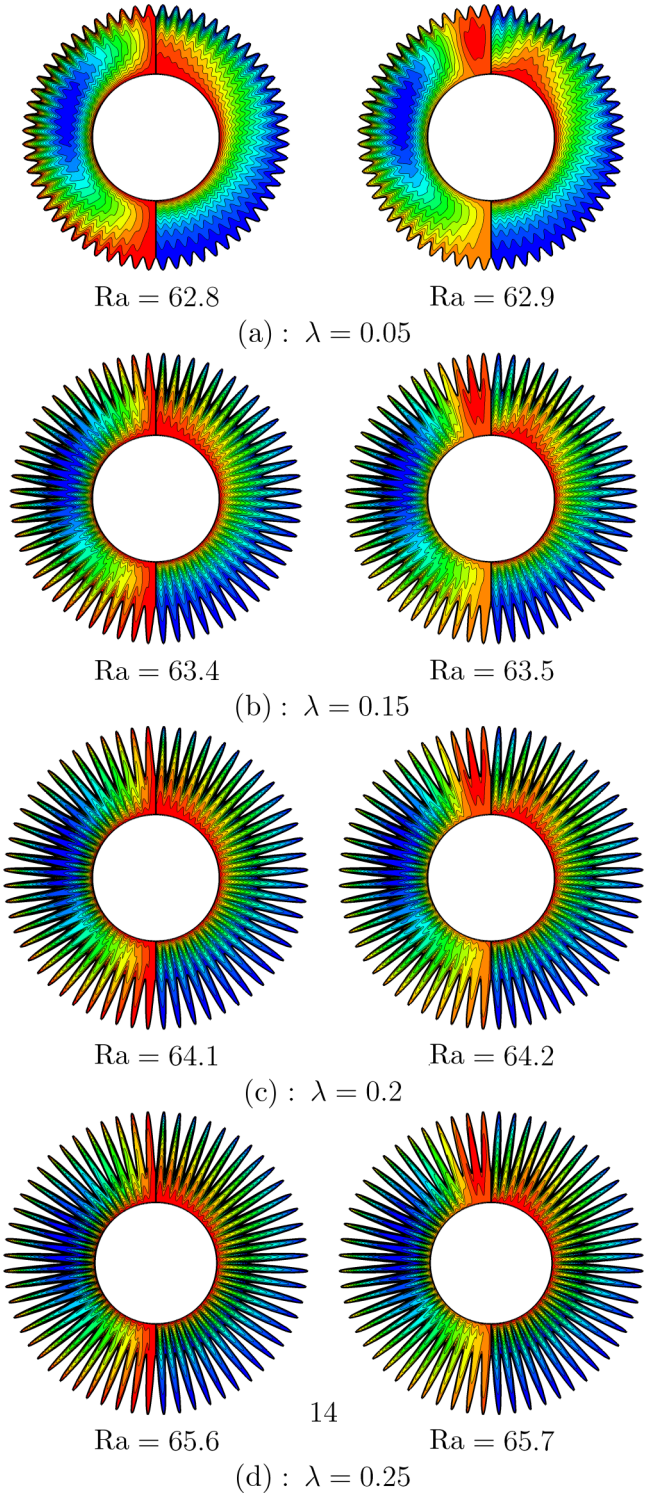

FIG. 4. Streamlines (left) and isotherms (right) for $\eta = 30$ and different values of λ.

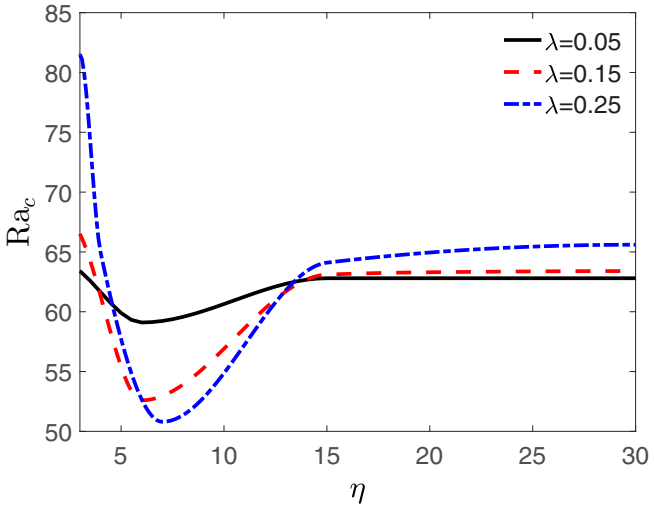

FIG. 5. Critical Rayleigh number as a function of undulation number for different λ.

The variation of the bifurcation point as a function of the undulation number for different values of the wavy wall amplitude is shown in Fig. 5. It is clearly noticed that the thermoconvective instabilities are more pronounced when the undulation number equals 6 and 7 for $\lambda < 0.25$ and $\lambda = 0.25$, respectively. It was also observed that, for $7 \leqslant \eta \leqslant 13$, the bifurcation point increases with the increase of the undulation number. However, for $\eta \geqslant 15$, no significant change on the thermoconvective instability is observed. Also, it is worth noting that the thermoconvective instabilities are more pronounced for high amplitudes when the undulation number is between 6 and 12. However, these instabilities are less pronounced for high amplitudes when $3 \leqslant \eta \leqslant 6$ or $\eta \geqslant 13$.

V. CONCLUSION

The thermal instability in a horizontal porous annulus with an external wavy wall has been studied. The porous matrix is supposed to be saturated by an incompressible fluid. The derived model with the temperature-stream function formulation is solved numerically using the finite difference alternating direction implicit method. Particular efforts have been focused on the effects of the Rayleigh number and the waviness of the external cylinder on the heat transfer and the flow pattern. Results show that the heat transfer and the convective instability depend on the waviness of the external wall. It has been found that the natural convection is an increasing function of the amplitude of sinusoidal profile. Moreover, one can conclude that the heat transfer increases with the undulation number when $\eta \leqslant 3$ and decreases for values of $\eta \geqslant 3$. It has been also shown that the thermoconvective instabilities are more pronounced with the undulation number when $3 \leqslant \eta \leqslant 6$. When the number of the undulation is between 7 and 12, the bifurcation point increases with η. It is also worth noting that exceeding a given threshold ($\eta = 15$), the number of undulations has no significant effect on the thermoconvective instabilities.

[1] J. P. Caltagirone, Thermoconvective instabilities in a porous medium bounded by two concentric horizontal cylinders, J. Fluid Mech. **76**, 337 (1976).

[2] J. Belabid and A. Cheddadi, Multicellular flows induced by natural convection in a porous horizontal cylindrical annulus, Phys. Chem. News **70**, 67 (2013).

[3] M. Charrier-Mojtabi, A. Mojtabi, M. Azaiez, and G. Labrosse, Numerical and experimental study of multicellular free convection flows in an annular porous layer, Int. J. Heat Mass Transf. **34**, 3061 (1991).
[4] M. C. Charrier-Mojtabi, Numerical simulation of two-and three-dimensional free convection flows in a horizontal porous annulus using a pressure and temperature formulation, Int. J. Heat Mass Transf. **40**, 1521 (1997).
[5] K. Himasekhar and H. H. Bau, Two-dimensional bifurcation phenomena in thermal convection in horizontal, concentric annuli containing saturated porous media, J. Fluid Mech. **187**, 267 (1988).
[6] Y. Rao, K. Fukuda, and S. Hasegawa, Steady and transient analyses of natural convection in a horizontal porous annulus with the Galerkin method, J. Heat Transf. **109**, 919 (1987).
[7] J. Belabid and K. Allali, Influence of gravitational modulation on natural convection in a horizontal porous annulus, J. Heat Transf. **139**, 022502 (2017).
[8] K. Khanafer, A. Al-Amiri, and I. Pop, Numerical analysis of natural convection heat transfer in a horizontal annulus partially filled with a fluid-saturated porous substrate, Int. J. Heat Mass Transf. **51**, 1613 (2008).
[9] H. F. Oztop, E. Abu-Nada, Y. Varol, and A. Chamkha, Natural convection in wavy enclosures with volumetric heat sources, Int. J. Thermal Sci. **50**, 502 (2011).
[10] B. R. Kumar, A study of free convection induced by a vertical wavy surface with heat flux in a porous enclosure, Numer. Heat Transf. A **37**, 493 (2000).
[11] M. A. Sheremet, C. Revnic, and I. Pop, Free convection in a porous wavy cavity filled with a nanofluid using Buongiorno's mathematical model with thermal dispersion effect, Appl. Math. Comput. **299**, 1 (2017).
[12] M. Hatami and D. Jing, Optimization of wavy direct absorber solar collector (WDASC) using Al_2O_3-water nanofluid and RSM analysis, Appl. Thermal Eng. **121**, 1040 (2017).
[13] M. Hassan, M. Marin, A. Alsharif, and R. Ellahi, Convective heat transfer flow of nanofluid in a porous medium over wavy surface, Phys. Lett. A **382**, 2749 (2018).
[14] A. Cheddadi, J. Caltagirone, A. Mojtabi, and K. Vafai, Free two-dimensional convective bifurcation in a horizontal annulus, J. Heat Transf. **114**, 99 (1992).
[15] J. B. Mota and E. Saatdjian, Natural convection in a porous, horizontal cylindrical annulus, J. Heat Transf. **116**, 621 (1994).
[16] G. Facas and B. Farouk, Transient and steady-state natural convection in a porous medium between two concentric cylinders, J. Heat Transf. **105**, 660 (1983).
[17] H. H. Bau, Thermal convection in a horizontal, eccentric annulus containing a saturated porous medium—An extended perturbation expansion, Int. J. Heat Mass Transf. **27**, 2277 (1984).
[18] G. N. Facas, Natural convection from a buried pipe with external baffles, Numer. Heat Transf. A **27**, 595 (1995).
[19] J. Mota, I. Esteves, C. Portugal, J. Esperança, and E. Saatdjian, Natural convection heat transfer in horizontal eccentric elliptic annuli containing saturated porous media, Int. J. Heat Mass Transf. **43**, 4367 (2000).
[20] A. F. Alfahaid, R. Sakr, and M. Ahmed, Natural convection heat transfer in concentric horizontal annuli containing a saturated porous media, IIUM Eng. J. **6**, 41 (2005).
[21] Z. Alloui and P. Vasseur, Natural convection in a horizontal annular porous cavity saturated by a binary mixture, Comput. Thermal Sci. **3**, 407 (2011).
[22] M. A. Sheremet and I. Pop, Free convection in a porous horizontal cylindrical annulus with a nanofluid using Buongiorno's model, Comput. Fluids **118**, 182 (2015).